Applied Energy 176 (2016) 22–33

Contents lists available at ScienceDirect

Applied Energy

journal homepage: www.elsevier.com/locate/apenergy

Comparative evaluation of GHG emissions from the use of *Miscanthus* for bio-hydrocarbon production *via* fast pyrolysis and bio-oil upgrading

Mobolaji B. Shemfe [a], Carly Whittaker [b], Sai Gu [c,*], Beatriz Fidalgo [a,*]

[a] Bioenergy & Resource Management Centre, Cranfield University, Bedford, Bedfordshire MK43 0AL, UK
[b] Agroecology Department, Rothamsted Research, Harpenden, Herts AL5 2JQ, UK
[c] Department of Chemical and Process Engineering, University of Surrey, Guildford, Surrey GU2 7XH, UK

HIGHLIGHTS

- GHG emissions from the upgrading of pyrolysis-derived bio-oil is quantified..
- Soil organic carbon sequestration rate had a significant effect on GHG emission.
- Increasing plant scale could improve the environmental performance of the system.
- Nitrogen to the pyrolysis reactor had significant impact on GHG emissions.

ARTICLE INFO

Article history:
Received 15 January 2016
Received in revised form 31 March 2016
Accepted 30 April 2016
Available online 13 May 2016

Keywords:
Fast pyrolysis
Biorefinery
GHG emissions
Bio-oil upgrading
Miscanthus
Life cycle assessment

ABSTRACT

This study examines the GHG emissions associated with producing bio-hydrocarbons *via* fast pyrolysis of *Miscanthus*. The feedstock is then upgraded to bio-oil products *via* hydroprocessing and zeolite cracking. Inventory data for this study were obtained from current commercial cultivation practices of *Miscanthus* in the UK and state-of-the-art process models developed in Aspen Plus®. The system boundary considered spans from the cultivation of *Miscanthus* to conversion of the pyrolysis-derived bio-oil into bio-hydrocarbons up to the refinery gate. The *Miscanthus* cultivation subsystem considers three scenarios for soil organic carbon (SOC) sequestration rates. These were assumed as follows: (i) excluding (SOC), (ii) low SOC and (iii) high (SOC) for best and worst cases. Overall, *Miscanthus* cultivation contributed moderate to negative values to GHG emissions, from analysis of excluding SOC to high SOC scenarios. Furthermore, the rate of SOC in the *Miscanthus* cultivation subsystem has significant effects on total GHG emissions. Where SOC is excluded, the fast pyrolysis subsystem shows the highest positive contribution to GHG emissions, while the credit for exported electricity was the main 'negative' GHG emission contributor for both upgrading pathways. Comparison between the bio-hydrocarbons produced from the two upgrading routes and fossil fuels indicates GHG emission savings between 68% and 87%. Sensitivity analysis reveals that bio-hydrocarbon yield and nitrogen gas feed to the fast pyrolysis reactor are the main parameters that influence the total GHG emissions for both pathways.

1. Introduction

Concern over global climate change due to increased anthropogenic greenhouse gas (GHG) emissions has prompted global action to limit the rise in global average temperature to 1.5 °C above pre-industrial levels [1]. CO_2 emissions attributed to fossil fuel combustion and industrial processes constitute 65% of total anthropogenic GHG emissions and are thus primary contributors. As a GHG mitigation strategy, biofuels are projected to contribute 27% of global transport fuel supply by 2050, with the aim of cutting CO_2 emissions by 2.1 Gt CO_2 eq per annum [2]. As part of the commitment to cut global GHG emissions, the EU has set a target to produce at least 10% of the energy used in the transport sector from renewable sources by 2020 [3]. In 2012, biofuels from food sources constituted 4.5% of road transport fuel supply in the EU. In 2015, the EU parliament progressed support for the use of sustainable biofuels in the transport sector, by placing a limit of 7% on biofuels from food crop sources as a means to enhance the production of advanced biofuels from non-food sources [4]. In the UK, road transport accounts for about 20% of total GHG emission, thus it is targeted for decarbonisation [5].

* Corresponding authors.
E-mail addresses: sai.gu@surrey.ac.uk (S. Gu), b.fidalgo@cranfield.ac.uk (B. Fidalgo).

http://dx.doi.org/10.1016/j.apenergy.2016.04.113
0306-2619/

Biofuels have been identified as one of several solutions for decarbonising the transport sector [6]. First generation biofuels derived from food crops currently constitute about 3% of global transport fuel demand [7]. However, they have been linked with sustainability issues, including the 'food vs. fuel' debate, as well as limited GHG emission savings and conflicting land use issues [8–10]. In order to avoid similar concerns, the development of new processes for the production of second generation biofuels from non-food sources, such as agricultural residues and dedicated energy crops, requires an adequate life cycle assessment (LCA) from an early stage prior to their commercial development.

Miscanthus has been identified as the most promising dedicated energy crop and a suitable candidate for the production of biofuels and biochemicals [11,12]. Trials have demonstrated high yields compared to other grasses [13], it shows low GHG emissions from cultivation [14] and displays high nutrient use efficiency [15]. Moreover, it tolerates low temperatures [16], is resistant to pests and diseases [13], and, as a C_4 grass is likely to utilise water more efficiently than C_3 bioenergy crops, such as reed canary grass and willow [17,18]. Approximately 8000 ha of *Miscanthus* are currently grown for bioenergy in England [19].

Fast pyrolysis is a promising thermochemical conversion process for producing advanced biofuels [20]. The process is achieved through the rapid thermal decomposition of biomass at temperatures between 450 and 600 °C, in the absence of oxygen to produce bio-oil, gas and char. Whilst the bio-oil product has been shown to have potential as a substitute fuel for boiler systems and stationary diesel engines, it is unsuitable for internal combustion engines due to its high oxygen content and low calorific value compared with conventional fossil fuels [20–25]. However, bio-oil can be upgraded into high-value hydrocarbons that can potentially complement or replace fossil fuel-derived equivalents [20,26,27].

Hydroprocessing and catalytic cracking are the two main processes for upgrading bio-oil into bio-hydrocarbons [20]. Hydroprocessing comprises two hydrogen-intensive and high-pressure operations *viz.* hydrodeoxygenation and hydrocracking. Hydrodeoxygenation involves the hydrocatalytic stabilisation and removal of oxygen atoms from oxygenates present in bio-oil at moderate operating pressures [28]. Hydrocracking occurs downstream of the hydrodeoxygenation operation at more severe pressures, to crack the heavy organic molecules of the hydrodeoxygenated bio-oil into shorter chain hydrocarbons, mainly consisting of aliphatics, naphthenes and aromatics [29–31]. On the other hand, catalytic cracking of bio-oil over zeolites occurs at atmospheric pressure in the absence of hydrogen to crack bio-oil molecules into lighter hydrocarbon species, predominantly aromatics and olefins [32,33]. The bio-hydrocarbon products from these upgrading processes are essential gasoline (petrol) and diesel blendstocks, and precursors for the production of high-value chemicals.

The prospect of producing bio-hydrocarbons from the fast pyrolysis of biomass and subsequent upgrading of the bio-oil product has prompted several life cycle assessment studies towards assessing the associated environmental impacts [34–39]. Hsu [34] reported that biofuels produced from fast pyrolysis of forest residues and bio-oil hydroprocessing reduced GHG emissions by 53% compared with conventional gasoline in a well-to-wheel (WTW) LCA study. In another study carried out by Iribarren et al. [35], 72% reduction in cradle-to-gate GHG emissions was reported for biofuels produced from fast pyrolysis of poplar and bio-oil hydroprocessing compared with fossil fuels equivalents. Zhang et al. [38] and Dang et al. [37] examined the net global warming potential (GWP) of biofuels from fast pyrolysis of corn stover and bio-oil hydroprocessing and reported GWP ranging from 69.1% to 147.5% for an array of process scenarios within a WTW system boundary. Han et al. [39] reported 60–112% reduction in WTW GHG emissions by substituting pyrolysis-derived fuels for fossil fuels based on various scenarios. Recently, Peters et al. [36] conducted a cradle-to-gate LCA study and revealed that GHG savings of 54.5% can be achieved by replacing conventional fuels with biofuels derived from fast pyrolysis of hybrid polar and bio-oil hydroprocessing. These studies considered bio-oil upgrading *via* hydroprocessing showing that hydroprocessing is an environmentally viable route for the production of second generation biofuels. Nevertheless, the quantification of the GHG emissions from the production of biofuels *via* the alternative upgrading process (zeolite cracking) is lacking in the open literature. At the time of writing, few published works address the LCA of biofuel production from the fast pyrolysis of perennial grasses such as *Miscanthus*. Moreover, it is important to understand the effect of soil organic carbon (SOC) sequestration in the *Miscanthus* cultivation stage on the overall GHG emissions of the two upgrading routes for real life applications. Understanding the impact of inventory selection and variables on GHG emissions in order to make effective decisions in real-time is also important for decision makers.

The aim of this work is to examine the GHG emissions from the use of *Miscanthus* to produce bio-hydrocarbons from fast pyrolysis and subsequent upgrading *via* hydroprocessing and zeolite cracking. The system boundary considered in this study spans from the cultivation of *Miscanthus* right to the conversion of pyrolysis-derived bio-oil into bio-hydrocarbons at the refinery gate. The contribution of each subsystem in the hydroprocessing and zeolite cracking conversion pathways to GHG emissions are individually quantified. Furthermore, the impact of three soil carbon sequestration scenarios on GHG emissions allocated to the *Miscanthus* cultivation subsystem is examined. Finally, sensitivity analyses are conducted to evaluate the influence of system parameters on total GHG emissions. It should be noted that the contribution of emissions from capital goods is not considered within the scope of this study, as they are suggested to have a negligible impact on LCA results [40,41].

2. Methods

2.1. LCA goal and scope

The goal of this study is to evaluate the GHG emissions that arise from the use of *Miscanthus* × *giganteus* to produce bio-hydrocarbons *via* fast pyrolysis and bio-oil upgrading. The functional unit is 1 tonne of bio-hydrocarbons produced from the 'cradle' to the refinery 'gate', and ready for distribution to the end user. Fig. 1 depicts the subsystems considered in this study within the cradle-to-gate system boundary. The subsystems considered include *Miscanthus* cultivation, *Miscanthus* transport, fast pyrolysis, and bio-oil upgrading. The supposed production site is located in Northwest England, therefore, inventory data and emission factors specific to the UK were employed. The GHG reporting methodology described in the European Commission's Renewable Energy Directive (RED) was followed. RED specifies that allocation between co-products should be performed *via* energy content in terms of lower heating value (LHV) and states that "GHG emission saving associated with excess electricity is equal to the amount of greenhouse gas that would be emitted when an equal amount of electricity is generated in a power plant using the same fuel as the cogeneration unit" [3]. In this work, the 'same fuel' refers to *Miscanthus*. As there are no dedicated *Miscanthus*-fired power stations in the UK, data was obtained from the Biomass Environmental Assessment Tool [42]. It was assumed that the thermal input rating of the plant is 40 MWth, net electrical output power rating is 10 MWe, the load factor is 85%, lifespan is 20 years, the conversion efficiency of the power plant is 25%, and 56.7 GJ of natural gas is required for power

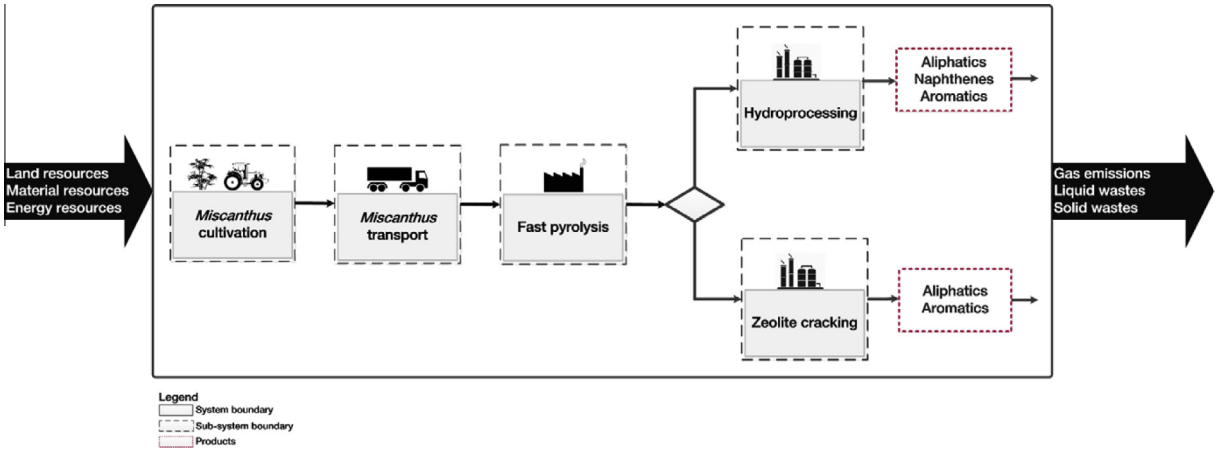

Fig. 1. Cradle-to-gate life cycle system of bio-hydrocarbon production from pyrolysis of *Miscanthus* and bio-oil upgrading.

plant start-up. Additionally, for consistency, it was assumed that the crop is transported to a similar distance to the theoretical *Miscanthus* power plant.

2.2. Inventory analysis

The inventory data used in this study is described in this section according to the different life cycle stages of the *Miscanthus* crop and conversion of *Miscanthus* into bio-hydrocarbons. The data for the life cycle stages of *Miscanthus* crop is based on the best available knowledge of production in the UK. The cropping system is representative of typical current commercial *Miscanthus* used for heat or power purposes [43]. Inventory data for the consumption of *Miscanthus* cultivation, including fertiliser, diesel and herbicides inputs were collected from industry experts, agricultural contractors and literature. Reliable inventory data for fast pyrolysis and upgrading subsystems are sparse in literature [35], and somewhat connected to the limited number of commercial-scale fast pyrolysis plants in operation to date [7]. Nevertheless, simulation results provide a reasonable estimate of the required inventory data. Thus, all previous LCA studies of biofuel production *via* fast pyrolysis [34–39] are mainly based on simulation results from process design and techno-economic studies [44–46]. Inventory data for the fast pyrolysis and upgrading subsystems in this study were obtained from simulation results from robust process models described elsewhere [47,48]. The procedures and methods used for acquiring the inventory data are detailed in the following subsections.

2.2.1. *Miscanthus* cultivation

Fig. 2 describes the processing steps in the *Miscanthus* cultivation subsystem.

2.2.1.1. Rhizome multiplication. *Miscanthus* rhizomes are currently commercially propagated in multiplication beds, where they are planted at densities of around 40,000 rhizomes/ha. Rhizomes are left for 2–6 years, depending on how successfully the stand grows, or on rhizome demand. Fertiliser input to the propagation sites depends on local soil fertility, as *Miscanthus* is a low input crop. Sites with poor fertility may show above-ground responses to nutrient addition [49], however, little is known about the effect on rhizome yield. A conservative estimate of 100 kg N/ha in the form of ammonium nitrate and 40 kg K_2O/ha in the form of potash was assumed. The contractors estimated that the farm machinery used in the entire process required between 480 and 670 l diesel/ha. A multiplication ratio of 1:14 was reported by the industry expert, although this ranges between 1:3 [50] (worse case) and 1:20 [51] (best case) in literature. The electricity demand was reported at 5.5 kW h/tonne rhizomes. The material from a typical site contains about one-third rhizome, the rest being soil and stones. The UK Department for Environment, Food & Rural Affairs (DEFRA) regulations specify that the soil and stones must be returned to the field [52].

2.2.1.2. Agronomy. The process of site establishment requires between 139 and 154 l diesel/ha, involving ploughing, power harrowing, planting, rolling and spraying. A typical planting density of 20,000 rhizomes/ha is practiced [19]. The contractors reported application rates of 6 kg a.i/ha during establishment, and 8 kg a.i/ha after the first cut, afterwards, leaf litter can effectively eliminate the need for weed control. Upon establishment, DEFRA's Fertiliser Manual of 2010 [52] recommends that very little N should be applied in the first two years as this encourages weed growth; instead, annual applications of 60–80 kg N/ha, in organic form, after years 2–3 are recommended. The organic fertiliser was assumed to be pig slurry, received from a local source 6.2 miles

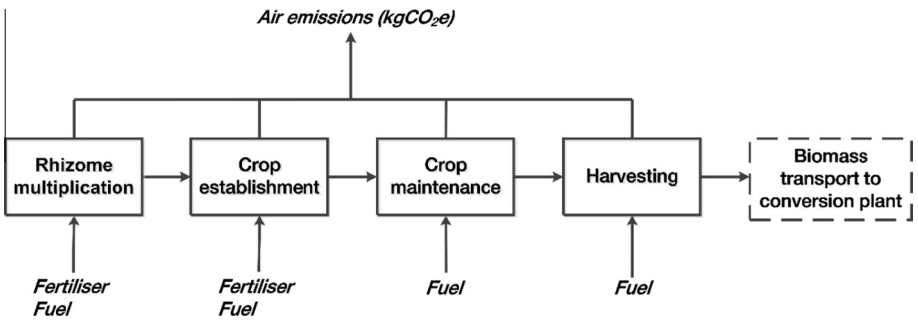

Fig. 2. *Miscanthus* cultivation subsystem.

(10 km), with a typical N, P and K nutrient content of 5 kg N/m^3, 1 kg P_2O_5/m^3 and 2.5 kg K_2O/m^3, respectively [53]. This was considered to be the 'worst-case' scenario as most commercial growers do not need to apply N to their crops (best scenario). Direct and indirect N_2O emission rates are expected to be the same as for arable crops, as demonstrated by experimental data [54].

First year maintenance requires around 7 l diesel/ha to cut back the first year's growth. *Miscanthus* harvests typically occur in the second year of growth. Forage harvesting requires between 15 and 26 l diesel/ha, depending on the type of cut and the thickness of crop. An estimate of 3.5 l/tonne was provided by the contractor for baling and movement to the roadside landing. Variation in *Miscanthus* yields has been attributed to climatic conditions, soil, water and nutrient availability, plant density, and harvest time [55]. The yield average includes the first year of no yield, a period of 3–5 years while the crop reaches its 'top yield' [56], a peak yield after about year 15, and then a slow decline of yield over the lifespan of the crop [57]. This study assumed a yield of 8–12 tonnes dry matter (DM)/ha/year in the worse and best case scenarios [18].

There is limited data available for crop termination as it is currently rarely carried out. In theory, the rhizome lifting process would not be performed on an old crop. In fact, the rhizome lifting process does not remove all rhizomes from the site. Current practice for complete eradication involves a subsoil operation and high herbicide (1–2 kg a.i/ha glyphosate) application.

Although crop establishment may cause oxidation of soil organic matter through ploughing [58], there is evidence that *Miscanthus* planted on arable land can increase the net SOC stored in the soil [14,59,60]. The extent of SOC sequestration depends on the original land use, harvest season, soil type and climate, as well as by the amount of crop residues left in the field and their turnover time [61]. In practice, collecting sufficient field samples to determine sequestration under crops is challenging, plus methodological variations such as sampling depth and fertilisation can obscure comparisons, and it is rare to find baseline soil carbon in which to compare with [62]. Based on a recent literature review [62], this study examined three scenarios: one excluding carbon sequestration to assess the GHG mitigation potential on supply chain GHG emissions alone, and two scenarios assuming low (0.42 tonnes C/ha/yr) and high (3.8 tonnes C/ha/yr) carbon sequestration rates. These were used to estimate the emission factors (EF) for the low and high case scenarios for SOC presented in Table 1. The inventory data for *Miscanthus* cultivation is summarised in Table 1.

2.2.2. Miscanthus transport

It was assumed that the *Miscanthus* is transported by 40-tonne trucks, each able to carry 25.5 tonnes at a 71% payload. The collection area was assumed to be within a 25-mile (40 km) radius from the conversion plant, where fast pyrolysis and bio-oil upgrading would take place. This assumption was based on the distance of 16–40 km between feedstock collection point and conversion plants encouraged by the UK government [66] as cited in [67]. The proposed fast pyrolysis plant is located in North-west England and supplied by high and medium-yield areas [68].

2.2.3. Fast pyrolysis subsystem

Fig. 3 illustrates the fast pyrolysis subsystem, which includes *Miscanthus* pretreatment, fast pyrolysis to produce bio-oil, char and non-condensable gas (NCG), and combustion of char and NCG to generate process heat and integrated electricity. Details of the simulation model of this section developed in Aspen plus® can be found elsewhere [47]. The model was verified and validated against experimental data to ensure its integrity [69]. A brief

Table 1
Inventory data for *Miscanthus* cultivation.

Item	Amount	Unit	EF	EF unit
Rhizome multiplication				
Inputs				
Rhizome	20,000 [19]	Rhizome/ha	–	[a]
Ammonium nitrate	100	kg N/ha	8.6	kg CO_2 eq./kg N [63]
Potash	40	kg K_2O/ha	0.6	kg CO_2 eq./kg K_2O [63]
Diesel	480–670	dm^3/ha	2.6	kg CO_2 eq./dm^3
Electricity	5.5	kW h	0.12	kg CO_2 eq./kW h [64]
Agronomy				
Inputs				
Rhizome input	20,000 [19]	Rhizome/ha	35–618	kg CO_2 eq./ha[b]
Site establishment	139–154	dm^3/ha	2.6	kg CO_2 eq./dm^3
Herbicide	6–8	kg a.i /ha	4.92	kg CO_2 eq./kg a.i [65]
Organic fertilizer	60–80	kg N/ha	4.3	kg CO_2 eq./kg a.i[c]
First-year maintenance	7	dm^3/ha	As above	
Harvesting	15–26	dm^3/ha		
Bailing and movement	3.5	dm^3/tonne		
Outputs				
Best-case scenario				
Miscanthus yield	12.8 [18]	ODT/ha yr[d]		
Excluding SOC	–	–	10.7	kg CO_2 eq./ODT
Low SOC	–	–	−41.8	kg CO_2 eq./ODT
High SOC	–	–	−464.3	kg CO_2 eq./ODT
Worst-case scenario				
Miscanthus yield	8 [18]	ODT/ha yr		
Excluding SOC	–	–	113	kg CO_2 eq./ODT
Low SOC	–	–	80.7	kg CO_2 eq./ODT
High SOC	–	–	−183.4	kg CO_2 eq./ODT

[a] Assume original rhizomes have a negligible impact.
[b] Based on separate rhizome multiplication analysis.
[c] Based on 10 km delivery and an N content 5 kg/m^3 slurry.
[d] ODT = oven dry tonne.

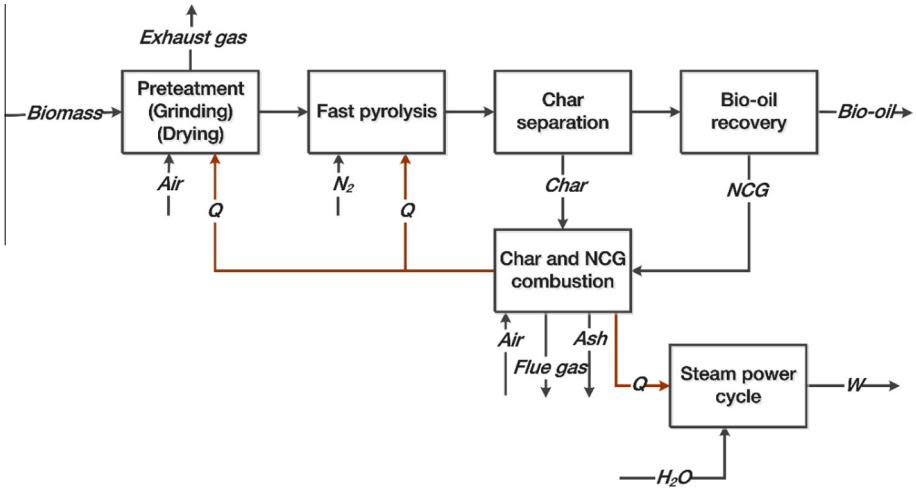

Fig. 3. Fast pyrolysis subsystem.

description of the fast pyrolysis subsystem is presented in Fig. 3, and its processing steps are discussed in the following subsections.

2.2.3.1. Pretreatment. In the pretreatment step, *Miscanthus* feedstock undergoes grinding operation to reduce its particle size to 2 mm, followed by a screen for particle separation. The particle size of the supplied feedstock was assumed to be 10 mm. The reduced particle size of the feedstocks enables effective mass and heat transfer in the dryer [70] and promotes rapid reaction in the fast pyrolysis reactor [20], although the latter depends on reactor configuration. The exiting *Miscanthus* stream with an assumed initial moisture content of 25 wt.% is then fed to a dryer to reduce its moisture content to 10 wt.%.

2.2.3.2. Fast pyrolysis. Next, the pre-treated biomass is converted into NCG, bio-vapours and solids (char and ash) inside the fast pyrolysis reactor, which was modelled as a bubbling fluidised bed reactor. Fluidisation of the reactor bed is aided by inert nitrogen gas. It was assumed that the nitrogen gas was supplied from a nearby installation *via* pressure swing adsorption (PSA). A purity of 99.5% was assumed, requiring approximately 383 kW h/tonne N_2 [71]. The fast pyrolysis model was based on chemical reaction kinetics [72] of the three biopolymer components of biomass: cellulose, hemicellulose and lignin. Table 2 outlines the biopolymer composition of *Miscanthus* employed in this study.

2.2.3.3. Product separation. Products from the pyrolysis reactor including, bio-vapours, NCG and solids are sent into a cyclone, where the solids are isolated from the product mixture. The exiting NCG and vapours from the cyclone then go into a quench system, which was modelled as a spray tower. In the spray tower, the hot bio-vapours are quenched into bio-oil. Subsequently, NCG and char are sent to the combustion section, while bio-oil is transferred to the upgrading subsystem. The recovered bio-oil product is transferred to the upgrading subsystems, which were assumed to be situated in the same location as the fast pyrolysis subsystem.

Table 2
Chemical composition of *Miscanthus* [12].

Subcomponent composition	wt.%
Cellulose	52.13
Hemicellulose	25.76
Lignin	12.58
Ash	2.47

2.2.3.4. Combustion and power generation. In the combustion section, NCG and char are combusted to generate process heat for drying operation and the pyrolysis reactor. The emissions and waste from the combustion section include hot flue gas and ash. It was assumed that the ash is landfilled, though there may be opportunities to use it as a substitute for agricultural limestone. The residual heat from combustion is used to produce superheated steam for electric power generation in an integrated steam cycle.

Table 3 summarises the inventory data obtained from the simulation model of the fast pyrolysis subsystem.

2.2.4. Bio-oil upgrading subsystems

Two bio-oil upgrading pathways were explored in this study *viz.* hydroprocessing and zeolite cracking.

Table 3
Daily inventory data for fast pyrolysis subsystem.

Item	Amount	Unit	EF	EF unit
Pretreatment				
Input				
Miscanthus	72	tonnes	–	–
Electricity for pretreatment	2424	kW h	0.12	kg CO_2 eq./kW h[a]
Output				
Pre-treated *Miscanthus*	59.8	tonnes	–	–
Fast pyrolysis				
Input				
Pre-treated *Miscanthus*	59.8	tonnes	–	–
Nitrogen	59.8	tonnes	–	–
Electricity for F.P	312	kW h	0.12	kg CO_2 eq./kW h [73]
N_2 gas	383	kW h/tonne	131	kg CO_2 eq./tonne [71]
Output				
Bio-oil	38.6	tonnes	–	–
Bio-char	8.1	tonnes	–	–
NCG	73.1	tonnes	–	–
Electricity	5,760	kW h	–	–
Ash to landfill	0.41	tonnes	0.09	kg CO_2 eq./tonne mile [42]

[a] Based on an onsite generator providing electricity from combustibles and biochar, assuming combustion emissions based on [73] for biomass, assuming CO_2 is neutral.

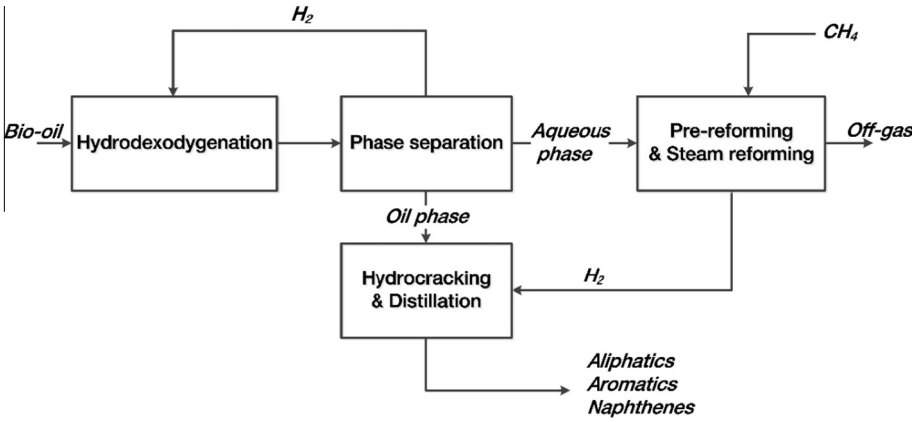

Fig. 4. Bio-oil hydroprocessing subsystem.

2.2.4.1. Bio-oil hydroprocessing. Fig. 4 illustrates bio-oil upgrading *via* the hydroprocessing route, which includes hydrodeoxygenation and hydrocracking of bio-oil, pre-reforming of the aqueous phase of the bio-oil and steam reforming of methane for the production of H_2, and final distillation of the oil phase into bio-hydrocarbons.

Details of the simulation model for this section developed in Aspen plus® can be found in earlier published studies [47,74]. The hydrodeoxygenation (HDO) of bio-oil occurs in two stages over Pt/Al_2O_3 catalyst as it produces more yields compared with conventional catalysts, such as sulfided $NiMo/Al_2O_3$ and $CoMo/Al_2O_3$ [75]. Due to lack of data for a specific emission factor for the Pt/Al_2O_3 catalyst, a crude estimate of 5 wt.% platinum/95 wt.% aluminium oxide composition was assumed [63,76]. The significance of this assumption is examined in the sensitivity analysis in Section 3.2. The hydrodeoxygenation reaction was based on a *pseudo*-first order kinetic model of lumped bio-oil components and was validated against reported experimental measurements [75]. The bio-oil obtained from the HDO process is separated into an aqueous phase and an oil phase. This study assumed that 40 wt.% of the aqueous phase of the bio-oil was pre-reformed along with steam reforming of supplementary methane to produce the hydrogen required in the hydrodeoxygenation and hydrocracking processing steps [77]. Although in theory 100 wt.% of the bio-oil aqueous phase can be pre-reformed to reduce the amount of supplementary methane, it is not practical because the high number of heavy organic sugar molecules present in the aqueous phase will likely lead to severe tar and coke formation at typical reforming temperatures [78]. The remaining bio-oil aqueous phase was assumed to be treated in a local wastewater treatment plant, where an electricity requirement of 1 kW h/m^3 is required for processing [79]. The oil phase undergoes hydrocracking under NiMo catalyst, and then the product is distilled to obtain gasoline and diesel range products. The total fuel yield is 14.16 t/day, mainly comprising of aromatics, naphthenes and n/i-alkanes of 12 wt.%, 70 wt.%, 18 wt.%, respectively. Table 4 summarises inventory data for the bio-oil hydroprocessing subsystem.

Table 4
Inventory data for bio-oil hydroprocessing subsystem.

Item	Amount	Unit	EF	EF unit
Input				
Bio-oil	38.60	tonnes	–	–
Methane	7.20	tonnes	2726	kg CO_2 eq./tonne [64]
Electricity	3312	kW h	0.12	kg CO_2 eq./kW h [73]
$Pt_2Al_2O_3$ catalyst	0.0053	tonnes	2596	kg CO_2 eq./tonne [63,80]
NiMo catalyst	0.0033	tonnes	8551	kg CO_2 eq./tonne [81]
Ni catalyst	0.0033	tonnes	8551	kg CO_2 eq./tonne [80]
Output				
Bio-hydrocarbons	14.16	tonnes	–	–
Aromatics	1.70	tonnes	–	–
Naphthenes	9.91	tonnes	–	–
n/i-alkanes	2.55	tonnes	–	–
Aqueous phase to treatment plant	11.76	tonnes	0.342	kg CO_2 eq./tonne [79]

2.2.4.2. Bio-oil zeolite cracking. The bio-oil upgrading *via* zeolite cracking is shown in Fig. 5.

Dehydration, cracking, deoxygenation and polymerisation reactions occur over H-ZSM5 catalyst in the zeolite reactor to produce hydrocarbon-rich-organic vapours, coke and gas. Product distribution was based on experimental results reported in literature [82,83] due to lack of reliable chemical reaction kinetic models. Emission factor for H-ZSM5 catalyst was derived from the GREET model [76]. The products from the zeolite cracking reactor then go into the product separation section. In this section, entrained catalyst in the gas product is separated by high-efficiency cyclones and charged along with spent catalyst into the regenerator.

The regenerator configuration considered in this study is a single stage regenerator fitted with a catalyst cooler. The spent catalyst is regenerated by complete combustion of coke, which results in severe temperatures in the regenerator. In order to avoid rapid catalyst deactivation that occurs at extreme temperatures [84], the regenerator temperature is regulated by a catalyst cooler, which exchanges heat with H_2O to generate superheated steam for subsequent electricity generation. The regenerated catalyst, carrying sufficient heat, is then charged back to the zeolite reactor to provide process heat.

The remaining stream of hot vapours and gas is quenched and sent to a flash drum to separate the product stream into gas, an aqueous phase (mainly H_2O) and an organic phase. The aqueous phase from the process was assumed to be delivered to a local wastewater treatment plant based on the same assumption made for the bio-oil hydroprocessing pathway [79]. The organic phase is finally sent to a distillation column to obtain bio-hydrocarbon products. The total fuel yield for zeolite cracking is 10.75 t/day, mainly comprising of 95 wt.% aromatics and 1.75 wt.% aliphatics. The heavy residue product (mainly carbon solid) from the distillation column was assumed as a co-product, which can be used for the production of graphite. Table 5 summarises inventory data for the bio-oil zeolite subsystem.

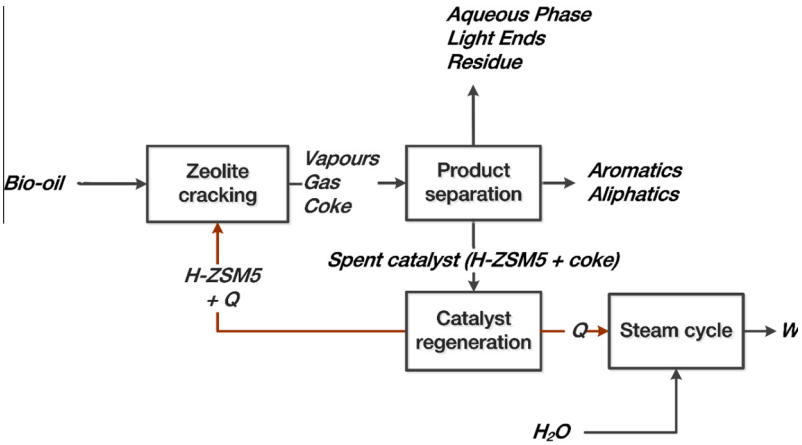

Fig. 5. Bio-oil zeolite upgrading subsystem.

Table 5
Daily inventory data for bio-oil zeolite cracking subsystem.

Item	Amount	Unit	EF	EF unit
Input				
Bio-oil	38.60	tonnes		
Electricity	3312	kW h	0.12	kg CO_2 eq./kW h [73]
HZSM-5 catalyst	0.0053	tonnes	7316	kg CO_2 eq./tonne [80]
Output				
Bio-hydrocarbons	11.74	tonnes	–	–
Electricity	17,928	kW h	–	–
CH_4	0.04	tonnes	–	–
C_2H_4	0.25	tonnes	–	–
C_3H_8	0.19	tonnes	–	–
C_4H_{12}	0.03	tonnes	–	–
C_4H_{10}	0.01	tonnes	–	–
C_2H_{12}	0.01	tonnes	–	–
Residue	1.728	tonnes	–	–
Wastewater to treatment plant	13.24	tonnes	0.342	kg CO_2 eq./tonne [79]

2.3. Methodology for emission allocation

The emission allocation procedure in the European Commission's Renewable Energy Directive (RED) was followed. RED stipulates that for multi-product systems, allocation of emissions have to be specified between the biofuel product and its co-products in proportion to their energy content (LHV). Allocation only occurs between co-products that are produced during the process and are not recycled to provide heat or power. For example, after pyrolysis co-products (NCG and char) are recycled into the process for combustion. Otherwise, allocation occurs at the point where the co-products are formed. This is the case of the zeolite upgrading of bio-oil in which the emissions are calculated after the co-products of the zeolite upgrading process (aqueous phase, light ends and residue) are formed. Following these fundamental allocation rules, the percentage allocation at each of the process stages in the subsystems were calculated using mass flows and the LHV of their respective products.

2.4. Sensitivity analysis

Sensitivity analysis was performed to evaluate the influence of variations in the input parameters to the subsystems in the two bio-hydrocarbon production pathways on GHG emissions. This provides an indication of the sensitivity of baseline GHG emissions to uncertainties or changes in input parameters. A variation range of ±50% was adopted for the sensitivity analysis.

3. Results and discussion

3.1. GHG emissions

3.1.1. GHG emissions bio-hydrocarbon production via hydroprocessing

The allocated GHG emissions to each subsystem in the hydroprocessing pathway based on different SOC scenarios is shown in Table 6.

Fig. 6 graphically compares the emission contribution of each subsystem to total GHG emissions of the different SOC scenarios.

As expected, the rate of SOC had a pronounced effect on emissions allocated to the *Miscanthus* cultivation subsystem and showed no impact on emissions assigned to the other subsystems in both the best and worst SOC cases. It can be seen in Fig. 6 that the best and worst-case scenarios for cultivation (excluding SOC) had a relatively small difference in the results. In contrast, the rate of SOC in the *Miscanthus* cultivation subsystem had a significant impact on the overall GHG emissions. The best-case excluding SOC was assumed as the 'industry standard' and used as the basis for further analysis.

According to the extent of GHG contribution, the key contributors were fast pyrolysis, bio-oil hydroprocessing and *Miscanthus* cultivation, contributing 74%, 13% and 9%, respectively. On the other hand, *Miscanthus* transport, *Miscanthus* pretreatment and waste processing steps had minimal contributions of 4%, 3% and

Table 6
Emission allocation for 1 tonne of bio-hydrocarbon produced for the hydroprocessing route.

Subsystem	Allocated emissions (kg CO_2 eq./t bio-hydrocarbon)					
	Worst case			Best case		
	Exclu SOC	Low SOC	High SOC	Exclu SOC[a]	Low SOC	High SOC
Cultivation	385	274	−622	36	−142	−1574
Transport	17	17	17	17	17	17
Fast pyrolysis	284	284	284	284	284	284
Pretreatment	10	10	10	10	10	10
Fast pyrolysis step	287	287	287	287	287	287
Electricity credit	−13	−13	−13	−13	−13	−13
Hydroprocessing	52	52	52	52	52	52
Hydroprocessing step	52	52	52	52	52	52
Waste processing	0.15	0.15	0.15	0.15	0.15	0.15
Total emission	738	627	−268	390	212	−1221

[a] Base case: excluding SOC best case scenario.

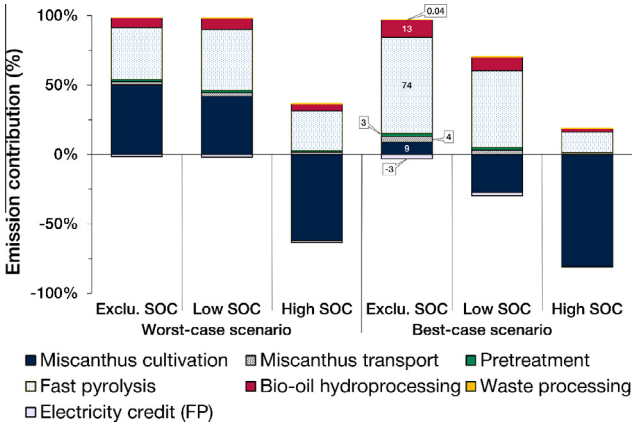

Fig. 6. Percentage contribution of subsystems in the hydroprocessing pathway to GHG emissions (FP denote electricity generated fast pyrolysis).

0.04%, respectively to GHG emissions. Electricity generated in the fast pyrolysis subsystem gave rise to 3% credit.

It is evident in Fig. 6 that the emission contribution of fast pyrolysis at 74%, clearly dominates the rest of the subsystems. This was attributed to electricity consumption in the PSA process for the production of feed N_2 to the pyrolysis reactor. Thus, the use of a different fluidising gas with less electricity requirement or carbon footprint in the pyrolysis reactor could reduce the emission contribution of the fast pyrolysis subsystem. The recycling of NCG back to the pyrolysis reactor to aid fluidisation has been suggested for industrial applications and has shown favourable results in experiments [85,86]. However, this would lead to a penalty in the amount of heat produced in the combustion section and the consequential electricity credit. Alternatively, air separation technologies different from the PSA process with less energy requirements [87], such as cryogenic distillation, could be employed for the production of N_2. Another possible solution is to use a different fast pyrolysis reactor configuration that excludes the need for a fluidising gas, such as the ablative, auger and vacuum moving bed reactor configurations. However, it is worth noting that these reactor configurations have been associated with unique operational problems and scale-up issues, including ineffective mass and heat transfer, limited heat supply, susceptibility to mechanical wear and process control difficulties [20]. The second significant contributor to GHG emissions was bio-oil hydroprocessing at 13%, mainly due to the amount of supplementary methane gas consumed in steam reforming for the production of hydrogen. A sensitivity analysis subsequently addresses the impact of methane gas on total GHG emissions in Section 3.2. The *Miscanthus* cultivation subsystem had a 9% contribution to total GHG emissions. The defining contributor to emissions in the *Miscanthus* cultivation subsystem is the rate of SOC sequestration as illustrated in Table 6. Furthermore, the rate of SOC visibly affects the percentage contribution of the other subsystems to total GHG emissions, moving from the scenarios excluding SOC to the scenarios with high SOC for worst and best cases as illustrated in Fig. 6. This result reinforces the proposition that *Miscanthus* is a suitable bioenergy crop for the production of bio-hydrocarbons. Although it is not yet well understood how much carbon is retained when the crops are terminated [57], it is likely that crop termination will lead to the decomposition of rhizomes and roots, releasing accumulated carbon as CO_2. It is also possible, that if the site is then re-planted with *Miscanthus* the previous level of sequestration could be restored, however, it will reach a similar saturation point [88]. The transport of *Miscanthus* contributed 4%, based on the 25-mile (40 km) distance assumed between the conversion plant and the *Miscanthus* collection site. *Miscanthus* pretreatment stage had a minimal contribution of 3% to the total GHG emissions. Emission contribution from this processing stage was attributed to the electricity consumed by dryer air compressor. Therefore, natural drying of the *Miscanthus* feed at storage prior to conversion would be environmentally efficient, although this has a minimal impact on total GHG contribution. Waste water processing had a negligible contribution of 0.04% to total GHG emissions. Electricity generation achieved 3% from the combustion of char and NCG.

3.1.2. GHG emissions from bio-oil zeolite cracking

Table 7 shows the allocated GHG emissions to each subsystem in the zeolite cracking pathway based on different SOC scenarios.

The emission contribution of each subsystem to total GHG emissions of the different SOC scenarios is portrayed in Fig. 7. For the base case, emission contribution in the order of impact, includes the fast pyrolysis step, *Miscanthus* cultivation, *Miscanthus* transport, zeolite cracking step, pretreatment and waste processing, with contributions of 92%, 12%, 6%, 5%, 3% and 0.05%, respectively. Electricity generated in the fast pyrolysis subsystem gave rise to 4% and 13% credit, respectively.

The emission contribution of each subsystem in the zeolite cracking pathway showed a similar trend to that observed in the

Table 7
Emission allocation for 1 tonne of bio-hydrocarbon produced for the zeolite pathway.

Subsystem	Allocated emissions (kg CO_2 eq./t bio-hydrocarbon)					
	Worst case			Best case		
	Exclu. SOC	Low SOC	High SOC	Exclu SOC[a]	Low SOC	High SOC
Cultivation	774	550	−1251	73	−285	−3167
Transport	35	35	35	35	35	35
Fast pyrolysis	571	571	571	571	571	571
Pretreatment	21	21	21	21	21	21
Fast pyrolysis step	577	577	577	577	577	577
Electricity credit	−26	−26	−26	−26	−26	−26
Zeolite cracking	−53	−53	−53	−53	−53	−53
Zeolite cracking step	28	28	28	28	28	28
Waste processing	0.32	0.32	0.32	0.32	0.32	0.32
Electricity credit	−81	−81	−81	−81	−81	−81
Total emission	1328	1104	−697	627	268	−2614

[a] Base case: excluding SOC best case scenario.

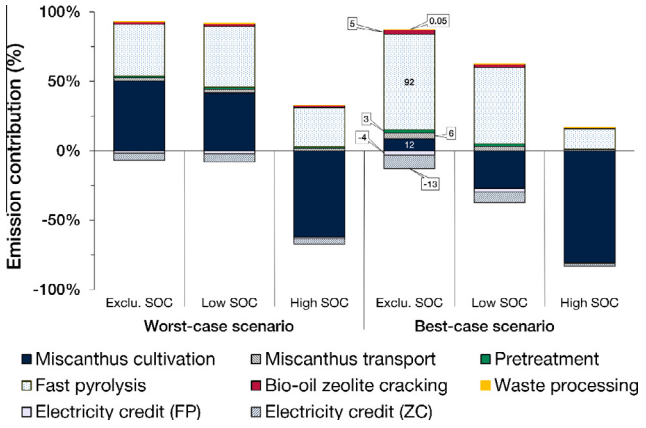

Fig. 7. Percentage contribution of subsystems in the hydroprocessing pathway to GHG emissions (ZC and FP denote electricity generated from zeolite cracking and fast pyrolysis, respectively).

hydroprocessing pathway with the exception of their respective upgrading subsystems. Lower emission contribution was seen in the zeolite upgrading subsystem in comparison with that observed in the hydroprocessing subsystem. This effect is due to neutral and negative emissions allocated to coke combustion and consequential electricity credits in the zeolite cracking subsystem, and the contributory positive emissions of supplementary methane in the hydroprocessing subsystem.

As the bio-hydrocarbons produced from the two upgrading pathways are not similar in composition, they were compared in terms of total CO_2 equivalent per energy content of their respective products for different SOC scenarios (see Fig. 8).

In addition, Fig. 9 shows the change in total GHG emissions from both pathways with respect to change in the emission factor of the *Miscanthus* cultivation subsystem due to SOC rates.

These results imply that the hydroprocessing pathway is more suitable for the sustainable production of bio-hydrocarbons than the zeolite pathway at excluding and low SOC rates. On the contrary, at high SOC rates the zeolite cracking pathway gradually becomes more suitable than the hydroprocessing pathway, because of its relatively higher rate of change (see Fig. 9).

3.2. Comparative GHG emissions with fossil fuels and other LCA studies

Although the scope of this work does not cover the ultimate use of the bio-hydrocarbon products, the results obtained give a good indication of the expected relative GHG emissions of both bio-oil upgrading pathways. WTW analysis is recommended when the end use of the bio-hydrocarbon products is for transport purposes. It is interesting to note that experimental studies on the blending limit of these bio-hydrocarbon products with fossil fuels up till now is limited, and thus could obscure reasonable WTW analysis and comparison. Moreover, it is important to account for the useful work done by the bio-hydrocarbon products in terms of vehicle operations in order to accurately account for the associated GHG emissions. Previous research in this field suggests that combustion of products from the hydroprocessing pathway in internal combustion engines will increase total WTW GHG emissions [34–36,38]. Alternatively, the bio-hydrocarbons produced from these pathways may be better suited as feedstocks for the petrochemical industry.

In order to conduct a baseline comparison with fossil fuels, GHG emissions from the bio-hydrocarbons when in use is taken as zero as specified in the RED methodology. Fig. 10 depicts the percentage emissions savings achievable from the bio-hydrocarbons produced from the hydroprocessing and zeolite cracking pathways in place of conventional fossil fuels, assuming direct emissions from the combustion of the bio-hydrocarbons is equal to zero. The fossil fuels for comparison include 100% mineral diesel, 100% mineral petrol (gasoline), CNG and LNG based on emission factors obtained from DEFRA [89].

The dashed line in Fig. 10 denotes the RED emission saving target, which mandates that as from 2017 biofuel installations will have to meet 60% GHG emissions savings in comparison with fossil fuels [90]. As shown in Fig. 10, both bio-hydrocarbons produced *via* the hydroprocessing and zeolite cracking pathways led to emissions savings above the RED target. The emissions savings achievable by replacing the fossil fuel comparators with bio-hydrocarbons obtained from the hydroprocessing route ranged from 87% to 82%. On the other hand, the emissions savings from substituting zeolite cracking-derived bio-hydrocarbons for fossil fuel comparators ranged from 77% to 68%. All in all, bio-hydrocarbons from the bio-oil hydroprocessing route showed 13–20% more emissions savings than those achieved from the zeolite cracking pathway.

The percentage GHG emission savings achievable by substituting bio-hydrocarbons derived from hydroprocessing with petrol (gasoline) is somewhat higher than reported values by other authors [34–38]. This moderate discrepancy is likely due to differences in the quality of data used for inventory assessment, scope of study, and methodologies for GHG calculations. Nevertheless, the value obtained in this study for GHG emission savings from substituting bio-hydrocarbons produced *via* the bio-oil hydroprocessing with petrol falls within the range of reported GHG savings of 60–112% reported by Han et al. [39] for various production scenarios. No appropriate comparison is possible in the case of zeolite upgrading of bio-oil as there is no present study on the GHG emissions of this process. Nevertheless, subsequent studies in this area should further validate the significance of the results presented in this study.

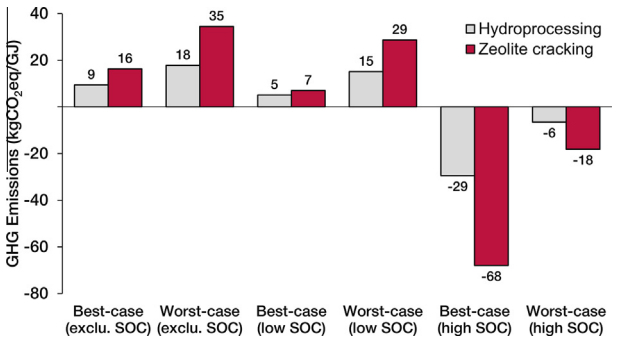

Fig. 8. Total GHG emissions (kg CO_2 eq./GJ) from hydroprocessing and zeolite cracking pathways for different SOC scenarios.

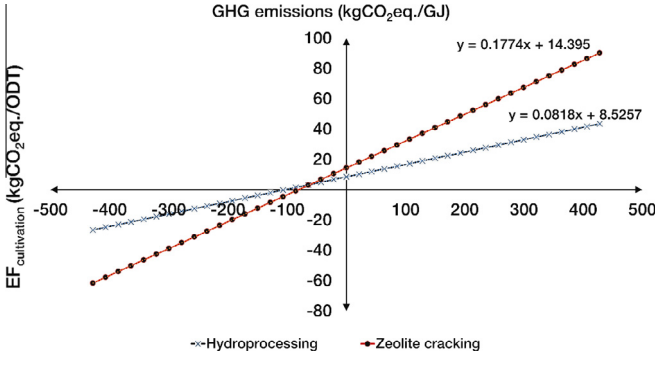

Fig. 9. Relationship between GHG emissions (kg CO_2 eq./GJ) from hydroprocessing and zeolite cracking pathways over a ±4000% change in base case emission factor in the cultivation subsystem.

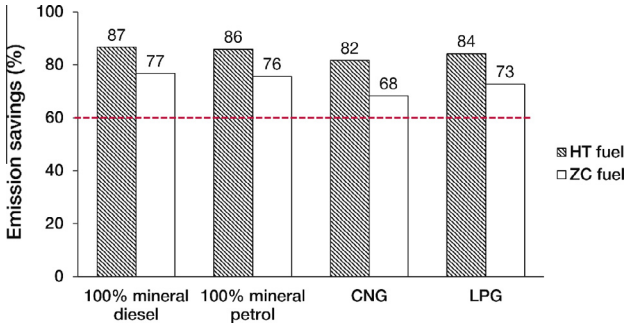

Fig. 10. Percentage emission savings of bio-hydrocarbons derived from bio-oil hydroprocessing (HT) and zeolite cracking (ZC) pathways compared to fossil fuels.

3.3. Sensitivity analysis

Figs. 11a and 11b illustrate the sensitivity of total GHG emissions (kg CO_2 eq./GJ) to ±50% variation in input parameters of the hydroprocessing pathway for the base case.

The sensitivity of total GHG emissions to variation in each parameter is denoted by the length of the bar charts from the baseline (9 kg CO_2 eq./GJ at 0%) in Fig. 11a. In addition, the trend of baseline GHG emissions to ±10% increments over the ±50% variation range is shown in Fig. 11b.

As shown in Figs. 11a and 11b, ±50% variation in bio-hydrocarbon yield and N_2 to the pyrolysis reactor had the most visible influence on total GHG emissions. Of these two, the bio-hydrocarbon yield had the highest impact. An increase of 50% in yield resulted in a 33% decrease in GHG emissions. Conversely, a reduction of 50% in yield led to a 100% increase in GHG emissions. This result suggests that attention should be paid to the bio-hydrocarbon yield, as a decrease in yield would result in a disproportionate increase in GHG emissions in comparison with the emission reduction of an increase in yield (see Fig. 11b). It is possible that the environmental performance of the system may benefit from economies of scale due to this effect.

An increase of 50% in N_2 gave rise to an increase of 33% in GHG emissions, and a decrease in yield resulted in a proportionate effect the other way round. This implies that careful consideration should be paid to the means of producing N_2. The utilisation of NCG for fluidisation has been suggested, and could prove to be a better choice for the environmental performance of the system. Moreover, a different reactor configuration could be utilised to exclude the use of N_2 in the pyrolysis reactor. Variation of ±50% in electricity generated in the fast pyrolysis subsystem, the distance between *Miscanthus* collection site and conversion plant, and methane to the steam reformer showed marginal effects on total GHG emissions. The most significant of these was electricity generated from the combustion of char and NCG in the fast pyrolysis subsystem. A decrease of 50% in electricity produced, led to a 10% increase in GHG emissions, while a 50% increase resulted in a reduction of 4%. The minimal impact of variation in electricity generated on total GHG emissions compared with the significant effects of variation in N_2 to the pyrolysis reactor appears to support the aforementioned suggestion of replacing N_2 with NCG. The distance between the *Miscanthus* collection point and the conversion plant and methane for reforming both had proportionate effects on GHG emissions when varied by ±50%. An increase of 50% in distance and methane led to an increase of 5% and 4% in emissions respectively and *vice versa*. The effect perceived in the variation in distance between the collection area and fast pyrolysis plant appears to justify the encouraged distance of 16–40 km by the UK government as GHG emissions increased linearly with distance as shown in Fig. 11b. Variation in methane for steam reforming showed moderate influence on total GHG emission. It is possible that integration of the steam reformer with downstream shift reactors to maximize the production of hydrogen could limit methane consumption, and consequently, reduce emissions. *Miscanthus* moisture content, Pt/Al_2O_3 catalyst, and electricity consumption in the pretreatment, fast pyrolysis and hydroprocessing steps had negligible impacts, of less than 2% on GHG emissions when varied in either direction.

In the same manner, Figs. 12a and 12b show the sensitivity of GHG emissions (kg CO_2 eq./GJ) to ±50% variation in input parameters of the zeolite cracking pathway. The value of the reference

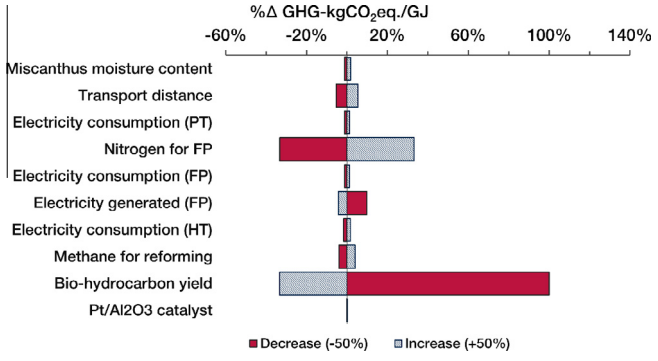

Fig. 11a. Sensitivity of GHG emissions (kg CO_2 eq./GJ) from hydroprocessing to ±50% variation in parameters (PT, FP and HT denote pretreatment, fast pyrolysis and hydroprocessing, respectively).

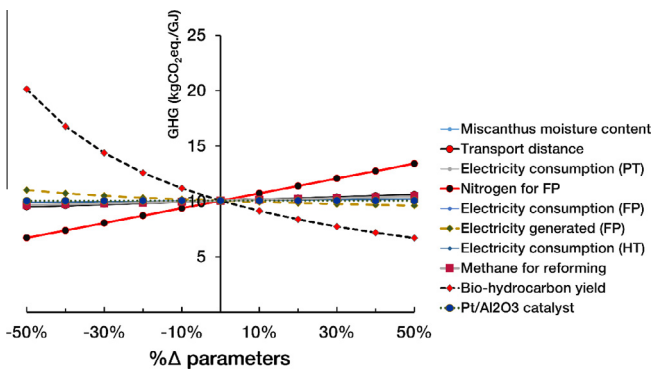

Fig. 11b. Trend of baseline GHG emissions from the hydroprocessing pathway over ±50% change in input parameters.

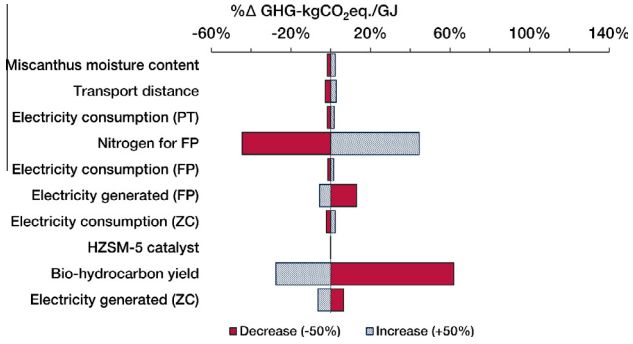

Fig. 12a. Sensitivity of GHG emissions (kg CO_2 eq./GJ) from the zeolite cracking pathway to ±50% variation in parameters (PT, FP and ZC denote pretreatment, fast pyrolysis and zeolite cracking, respectively).

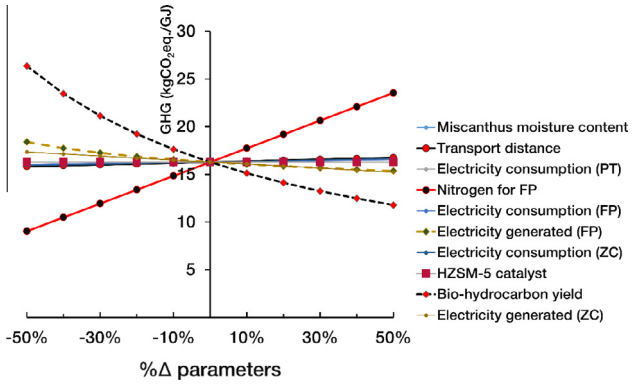

Fig. 12b. Trend of GHG emissions from the zeolite cracking pathway over ±50% change in input parameters.

point for the sensitivity analysis is 16 kg CO_2 eq./GJ. Overall, the sensitivity of the zeolite cracking pathway showed a similar trend to the observations in the hydroprocessing pathway, thus, the implications discussed above are applicable. Concisely, a variation of ±50% in bio-hydrocarbon yield and nitrogen gas for fast pyrolysis had the most impacts on GHG emissions.

Bio-hydrocarbon yield had the highest impact on GHG emissions with an increase of 50% in the yield producing a 28% reduction. On the other hand, a decrease of 50% in bio-hydrocarbon yield led to a 62% increase in GHG emissions. An increase of 50% in nitrogen gas feed give rise to a decline of 44% in GHG emissions and *vice versa*. The distance between the *Miscanthus* collection area and the fast pyrolysis plant showed 3% change to the baseline GHG emissions when increased by 50% and *vice versa*. The baseline GHG emissions showed 13% and 6% increases to 50% decrease in electricity generated by fast pyrolysis and zeolite cracking, respectively. Conversely, an increase of 50% in electricity generated in fast pyrolysis and zeolite cracking subsystems led to 5% and 6% decrease in GHG emissions, respectively. Variation of ±50% in the electricity consumption in the zeolite cracking, the pre-treatment and the fast pyrolysis steps, and *Miscanthus* moisture content had the lowest noticeable effects on GHG emissions ranging from ±1.5% to 2.3% when varied either way. HZSM-5 catalyst had negligible impacts of less than 1% when varied.

4. Conclusions

The GHG emissions that arise from the use of *Miscanthus* for the production of bio-hydrocarbons *via* fast pyrolysis and bio-oil hydroprocessing and zeolite cracking has been investigated. The results indicated that the fast pyrolysis subsystem was the major contributor to GHG emissions for both bio-oil hydroprocessing and zeolite cracking pathways in excluding SOC and low SOC scenarios. *Miscanthus* cultivation, *Miscanthus* transport and upgrading subsystems also had modest contributions to GHG emissions. In particular, the rate of SOC in the *Miscanthus* cultivation subsystem had a vast effect on net GHG savings. Bio-hydrocarbons produced from the two upgrading processes used as a substitute for fossil fuel equivalent resulted in more than 60% emission savings, which is the threshold mandated by the EU directive for new biofuel installations. Sensitivity analysis revealed that the GHG emission of both routes is mostly influenced by changes in bio-hydrocarbon yield and nitrogen feed gas for the fast pyrolysis reactor. Thus, particular attention should be paid to the means of producing nitrogen feed gas to the reactor. Evaluation of the impact of different pyrolysis reactor configurations on GHG emissions is suggested for further research. Additionally, probabilistic analysis to account for the characteristic uncertainties in the rate of SOC would give the range of confidence in the results.

Acknowledgements

The authors gratefully acknowledge the financial support for this work by the UK Engineering and Physical Sciences Research Council (EPSRC) project reference: EP/K036548/1 and FP7 Marie Curie iComFluid project reference: 312261.

References

[1] United Nations. Adoption of the Paris Agreement, vol. 21932. Paris, France; 2015.
[2] IEA. Technology roadmap: biofuels for transport. Paris, France: IEA Publications; 2011.
[3] European Commission. Directive 2009/28/EC of the European Parliament and of the Council of 23 April 2009 on the promotion of the use of energy from renewable sources. Brussels, Belgium; 2009.
[4] EBTP. European biofuels technology platform EBTP – overview and history n.d. <http://www.biofuelstp.eu/overview.html> [accessed December 31, 2015].
[5] DECC. 2013 UK greenhouse gas emissions, final figures statistical release; 2015.
[6] DTI. Meeting the energy challenge: a white paper on energy. London United Kingdom; 2007. http://dx.doi.org/10.1016/j.nucengdes.2006.02.017.
[7] IEA Bioenergy Task 39. The potential and challenges of "drop in" biofuels; 2014.
[8] Locke A, Henley G. A review of the literature on biofuels and food security at a local level; 2014.
[9] Naik SN, Goud VV, Rout PK, Dalai AK. Production of first and second generation biofuels: a comprehensive review. Renew Sustain Energy Rev 2010;14:578–97. http://dx.doi.org/10.1016/j.rser.2009.10.003.
[10] Sims RH, Mabee W, Saddler JN, Taylor M. An overview of second generation biofuel technologies. Bioresour Technol 2010;101:1570–80. http://dx.doi.org/10.1016/j.biortech.2009.11.046.
[11] Don A, Osborne B, Hastings A, Skiba U, Carter MS, Drewer J, et al. Land-use change to bioenergy production in Europe: implications for the greenhouse gas balance and soil carbon. GCB Bioenergy 2012;4:372–91. http://dx.doi.org/10.1111/j.1757-1707.2011.01116.x.
[12] Brosse N, Dufour A, Meng X, Sun Q, Ragauskas A. *Miscanthus*: a fast-growing crop for biofuels and chemicals production. Biofuels, Bioprod Biorefining 2012;6:580–98. http://dx.doi.org/10.1002/bbb.
[13] Riche AB. A trial of the suitability of switchgrass and reed canary grass as biofuel crops under UK conditions. Harpenden, UK: Rothamsted Research; 2005.
[14] Hillier J, Whittaker C, Dailey G, Aylott M, Casella E, Richter GM, et al. Greenhouse gas emissions from four bioenergy crops in England and Wales: integrating spatial estimates of yield and soil carbon balance in life cycle analyses. GCB Bioenergy 2009;1:267–81. http://dx.doi.org/10.1111/j.1757-1707.2009.01021.x.
[15] Cadoux S, Riche AB, Yates NE, Machet J-M. Nutrient requirements of *Miscanthus* x giganteus: conclusions from a review of published studies. Biomass Bioenergy 2012;38:14–22. http://dx.doi.org/10.1016/j.biombioe.2011.01.015.
[16] Farage PK, Blowers D, Long SP, Baker NR. Low growth temperatures modify the efficiency of light use by photosystem II for CO_2 assimilation in leaves of two chilling-tolerant C 4 species, *Cyperus longus* L. and *Miscanthus* × *giganteus*. Plant, Cell Environ 2006;29:720–8. http://dx.doi.org/10.1111/j.1365-3040.2005.01460.x.
[17] Hall RL. Grasses for energy production: hydrological guidelines; 2003.
[18] Richter GM, Riche AB, Dailey AG, Gezan SA, Powlson DS. Is UK biofuel supply from *Miscanthus* water-limited? Soil Use Manage 2008;24:235–45. http://dx.doi.org/10.1111/j.1475-2743.2008.00156.x.
[19] DEFRA. Planting and growing *Miscanthus*. London United Kingdom; 2007.
[20] Bridgwater AV. Review of fast pyrolysis of biomass and product upgrading. Biomass Bioenergy 2012;38:68–94. http://dx.doi.org/10.1016/j.biombioe.2011.01.048.
[21] Brown R, Holmgren J. Fast pyrolysis and bio-oil upgrading. Bioenergy Energy Altern Biomass Diesel Work; 2006.
[22] Bridgwater AV, Peacocke GVC. Fast pyrolysis processes for biomass. Renew Sustain Energy Rev 2000;4:1–73. http://dx.doi.org/10.1016/S1364-0321(99)00007-6.
[23] Bridgwater AV, Toft AJ, Brammer JG. A techno-economic comparison of power production by biomass fast pyrolysis with gasification and combustion, vol. 6; 2002. http://dx.doi.org/10.1016/S1364-0321(01)00010-7.
[24] Lehto J, Oasmaa A, Solantausta Y, Kytö M, Chiaramonti D. Review of fuel oil quality and combustion of fast pyrolysis bio-oils from lignocellulosic biomass. Appl Energy 2014;116:178–90. http://dx.doi.org/10.1016/j.apenergy.2013.11.040.
[25] Van de Beld B, Holle E, Florijn J. The use of pyrolysis oil and pyrolysis oil derived fuels in diesel engines for CHP applications. Appl Energy 2013;102:190–7. http://dx.doi.org/10.1016/j.apenergy.2012.05.047.
[26] Bridgwater AV. Upgrading biomass fast pyrolysis liquids. Environ Prog Sustain Energy 2012;31:261–8. http://dx.doi.org/10.1002/ep.11635.
[27] Xiu S, Shahbazi A. Bio-oil production and upgrading research: a review. Renew Sustain Energy Rev 2012;16:4406–14. http://dx.doi.org/10.1016/j.rser.2012.04.028.
[28] Demirbas A. Competitive liquid biofuels from biomass. Appl Energy 2011;88:17–28. http://dx.doi.org/10.1016/j.apenergy.2010.07.016.
[29] Elliott DC, Hart TR, Neuenschwander GG, Rotness LJ, Zacher AH. Catalytic hydroprocessing of biomass fast pyrolysis bio-oil to produce hydrocarbon products. Environ Prog Sustain Energy 2009;28:441–9. http://dx.doi.org/10.1002/ep.10384.
[30] Wang H, Male J, Wang Y. Recent advances in hydrotreating of pyrolysis bio-oil and its oxygen-containing model compounds. ACS Catal 2013;3:1047–70. http://dx.doi.org/10.1021/cs400069z.
[31] Elliott D. Advancement of bio-oil utilization for refinery feedstock. In: Washingt bioenergy res symp.
[32] Adjaye JD, Bakhshi NN. Catalytic conversion of a biomass-derived oil to fuels and chemicals I: model compound studies and reaction pathway. Biomass Bioenergy 1995;8:265–77. http://dx.doi.org/10.1016/0961-9534(95)00019-4.
[33] Tan S, Zhang Z, Jianping S, Wang Q. Recent progress of catalytic pyrolysis of biomass by HZSM-5. Chin J Catal 2013;34:641–50. http://dx.doi.org/10.1016/S1872-2067(12)60531-2.
[34] Hsu DD. Life cycle assessment of gasoline and diesel produced via fast pyrolysis and hydroprocessing. Golden, CO; 2011.

[35] Iribarren D, Peters JF, Dufour J. Life cycle assessment of transportation fuels from biomass pyrolysis. Fuel 2012;97:812–21. http://dx.doi.org/10.1016/j.fuel.2012.02.053.

[36] Peters JF, Iribarren D, Dufour J. Simulation and life cycle assessment of biofuel production via fast pyrolysis and hydroupgrading. Fuel 2015;139:441–56. http://dx.doi.org/10.1016/j.fuel.2014.09.014.

[37] Dang Q, Yu C, Luo Z. Environmental life cycle assessment of bio-fuel production via fast pyrolysis of corn stover and hydroprocessing. Fuel 2014;131:36–42. http://dx.doi.org/10.1016/j.fuel.2014.04.029.

[38] Zhang Y, Hu G, Brown RC. Life cycle assessment of the production of hydrogen and transportation fuels from corn stover via fast pyrolysis. Environ Res Lett 2013;8:025001. http://dx.doi.org/10.1088/1748-9326/8/2/025001.

[39] Han J, Elgowainy A, Dunn JB, Wang MQ. Life cycle analysis of fuel production from fast pyrolysis of biomass. Bioresour Technol 2013;133:421–8. http://dx.doi.org/10.1016/j.biortech.2013.01.141.

[40] Muench S, Guenther E. A systematic review of bioenergy life cycle assessments. Appl Energy 2013;112:257–73. http://dx.doi.org/10.1016/j.apenergy.2013.06.001.

[41] Luo L, Voet E, Huppes G, de Haes HA. Allocation issues in LCA methodology: a case study of corn stover-based fuel ethanol. Int J Life Cycle Assess 2009;14:529–39. http://dx.doi.org/10.1007/s11367-009-0112-6.

[42] DEFRA. Biomass environmental assessment tool (BEAT2). UK DEFRA; 2008.

[43] Whittaker C. The importance of life cycle assessment (LCA) | BioFina. University of Batth; 2013.

[44] Jones SB, Holladay JE, Valkenburg C, Stevens DJ, Walton CW, Kinchin C, et al. Production of gasoline and diesel from biomass via fast pyrolysis, hydrotreating and hydrocracking: a design case. Oakridge: PNNL; 2009.

[45] Wright MM, Daugaard D, Satrio JA, Brown R, Hsu D. Techno-economic analysis of biomass fast pyrolysis to transportation fuels. NREL Golden, CO; 2010. http://dx.doi.org/10.1016/j.fuel.2010.07.029.

[46] Peters JF, Iribarren D, Dufour J. Predictive pyrolysis process modelling in Aspen Plus. In: 21st Eur biomass conf exhib.

[47] Shemfe M, Gu S, Ranganathan P. Techno-economic performance analysis of biofuel production and miniature electric power generation from biomass fast pyrolysis and bio-oil upgrading. Fuel 2015;143:361–72. http://dx.doi.org/10.1016/j.fuel.2014.11.078.

[48] Shemfe MB, Gu S, Fidalgo B. The techno-economic potential of biofuel production via bio-oil zeolite upgrading: an evaluation of two catalyst regeneration systems. Energy; n.d.

[49] Shield IF, Barraclough TJP, Riche AB, Yates NE. The yield and quality response of the energy grass *Miscanthus* × *giganteus* to fertiliser applications of nitrogen, potassium and sulphur. Biomass Bioenergy 2014;68:185–94. http://dx.doi.org/10.1016/j.biombioe.2014.06.007.

[50] Atkinson CJ. Establishing perennial grass energy crops in the UK: a review of current propagation options for *Miscanthus*. Biomass Bioenergy 2009;33:752–9. http://dx.doi.org/10.1016/j.biombioe.2009.01.005.

[51] Bullard M, Metcalfe P. Estimating the energy requirements and CO_2 emissions from production of the perennial grasses: *Miscanthus*, switchgrass and reed canary grass; 2001.

[52] DEFRA. Fertiliser recommendations for agricultural and horticultural crops (RB209). London United Kingdom; 2010.

[53] Cavanagh A, Gasser MO, Labrecque M. Pig slurry as fertilizer on willow plantation. Biomass Bioenergy 2011;35:4165–73. http://dx.doi.org/10.1016/j.biombioe.2011.06.037.

[54] Drewer J, Finch JW, Lloyd CR, Baggs EM, Skiba U. How do soil emissions of N_2O, CH_4 and CO_2 from perennial bioenergy crops differ from arable annual crops? GCB Bioenergy 2012;4:408–19. http://dx.doi.org/10.1111/j.1757-1707.2011.01136.x.

[55] Danalatos NG, Archontoulis SV, Mitsios I. Potential growth and biomass productivity of *Miscanthus* × *giganteus* as affected by plant density and N-fertilization in central Greece. Biomass Bioenergy 2007;31:145–52. http://dx.doi.org/10.1016/j.biombioe.2006.07.004.

[56] Lewandowski I, Clifton-Brown JC, Scurlock JMO, Huisman W. *Miscanthus*: European experience with a novel energy crop. Biomass Bioenergy 2000;19:209–27. http://dx.doi.org/10.1016/S0961-9534(00)00032-5.

[57] Clifton-Brown J, Breuer J, Jones MB. Carbon mitigation by the energy crop, *Miscanthus*. Glob Chang Biol 2007;13:2296–307. http://dx.doi.org/10.1111/j.1365-2486.2007.01438.x.

[58] Murphy F, Devlin G, McDonnell K. *Miscanthus* production and processing in Ireland: an analysis of energy requirements and environmental impacts. Renew Sustain Energy Rev 2013;23:412–20. http://dx.doi.org/10.1016/j.rser.2013.01.058.

[59] Hamelin L, Jørgensen U, Petersen BM, Olesen JE, Wenzel H. Modelling the carbon and nitrogen balances of direct land use changes from energy crops in Denmark: a consequential life cycle inventory. GCB Bioenergy 2012;4:889–907. http://dx.doi.org/10.1111/j.1757-1707.2012.01174.x.

[60] Clair SS, Hillier J, Smith P. Estimating the pre-harvest greenhouse gas costs of energy crop production. Biomass Bioenergy 2008;32:442–52. http://dx.doi.org/10.1016/j.biombioe.2007.11.001.

[61] Foereid B, De Neergaard A, Høgh-Jensen H. Turnover of organic matter in a *Miscanthus* field: effect of time in Miscanthus cultivation and inorganic nitrogen supply. Soil Biol Biochem 2004;36:1075–85. http://dx.doi.org/10.1016/j.soilbio.2004.03.002.

[62] McCalmont JP, Hastings A, McNamara NP, Richter GM, Robson P, Donnison IS, et al. Environmental costs and benefits of growing *Miscanthus* for bioenergy in the UK. GCB Bioenergy 2015. http://dx.doi.org/10.1111/gcbb.12294.

[63] Swiss Centre for Life Cycle Inventories. Ecoinvent Database 2.2. Dubendorf, Switzerland; 2007.

[64] DEFRA. Carbon factors. London United Kingdom; n.d.

[65] Elsayed M, Matthews R, Mortimer N. Carbon and energy balances for a range of biofuels options. London UK; 2003.

[66] Rural development programme for England. Sheffield UK: Handbook, Energy Crops Scheme Establishment Grants; 2007.

[67] Thornley P. Airborne emissions from biomass based power generation systems. Environ Res Lett 2008;3:014004. http://dx.doi.org/10.1088/1748-9326/3/1/014004.

[68] DEFRA Industrial Crops – Archive: Opportunities and optimum sitings for energy crops <http://webarchive.nationalarchives.gov.uk/20130402151656/>, <http://archive.defra.gov.uk/foodfarm/growing/crops/industrial/energy/opportunities/nw.htm> [accessed December 13, 2015].

[69] Wang X, Kresten SRA, Prins W, Van Swaaij PMW. Biomass pyrolysis in a fluidized bed reactor. Part 2: Experimental validation of model results. Ind Eng Chem Res 2005:8786–95. http://dx.doi.org/10.1021/ie050486v.

[70] Li H, Chen Q, Zhang X, Finney KN, Sharifi VN, Swithenbank J. Evaluation of a biomass drying process using waste heat from process industries: a case study. Appl Therm Eng 2012;35:71–80. http://dx.doi.org/10.1016/j.applthermaleng.2011.10.009.

[71] Flowe Mike The Energy Costs Associated with Nitrogen Specifications | Compressed Air Best Practices <http://www.airbestpractices.com/system-assessments/air-treatmentn2/energy-costs-associated-nitrogen-specifications> [accessed December 18, 2015].

[72] Ranzi E, Faravelli T, Frassoldati A, Migliavacca G, Pierucci S, Sommariva S. Chemical kinetics of biomass pyrolysis. Energy Fuels 2008:4292. http://dx.doi.org/10.1021/ef800551t.

[73] Hagberg L, Särnholm E, Gode J, Ekvall T, Rydberg T. LCA calculations on Swedish wood pellet production chains; 2009. p. 1–61.

[74] Shemfe MB, Fidalgo B, Gu S. Heat integration for bio-oil hydroprocessing coupled with aqueous phase steam reforming. Chem Eng Res Des 2015. http://dx.doi.org/10.1016/j.cherd.2015.09.004.

[75] Sheu Y-HE, Anthony RG, Soltes EJ. Kinetic studies of upgrading pine pyrolytic oil by hydrotreatment. Fuel Process Technol 1988;19:31–50. http://dx.doi.org/10.1016/0378-3820(88)90084-7.

[76] Elgowainy A, Dieffenthaler D, Sokolov V, Sabbisetti R, Cooney C, Anjum A. GREET 2013; 2012.

[77] Marker TL, Petri JA. Gasoline and diesel production from pyrolytic lignin produced from pyrolysis of cellulosic waste; 2008.

[78] Marker TL. Opportunities for biorenewables in oil refineries Final technical report. United States. Des Plaines, IL: UOP; 2005.

[79] Helble A, Möbius CH. Current experience with the use of membrane bioreactor technology for the treatment of papermill effluent. In: PTS water environ technol symp, Munich Germany.

[80] Argonne National Laboratory. GREET model; n.d.

[81] Lavery N, Jarvis D, Brown SR, Adkins N, Wilson B. Life cycle assessment of sponge nickel produced by gas atomisation for use in industrial hydrogenation catalysis applications. Int J Life Cycle Assess 2013;18:362–76. http://dx.doi.org/10.1007/s11367-012-0478-8.

[82] Sharma RK, Bakhshi NN. Catalytic upgrading of fast pyrolysis oil over hzsm-5. Can J Chem Eng 1993;71:383–91. http://dx.doi.org/10.1002/cjce.5450710307.

[83] Adjaye JD, Katikaneni SPR, Bakhshi NN. Catalytic conversion of a biofuel to hydrocarbons: effect of mixtures of HZSM-5 and silica-alumina catalysts on product distribution. Fuel Process Technol 1996;48:115–43. http://dx.doi.org/10.1016/S0378-3820(96)01031-4.

[84] Talmadge MS, Baldwin RM, Biddy MJ, McCormick RL, Beckham GT, Ferguson GA, et al. A perspective on oxygenated species in the refinery integration of pyrolysis oil. Green Chem 2014;16:407. http://dx.doi.org/10.1039/c3gc41951g.

[85] Zhang H, Xiao R, Huang H, Xiao G. Comparison of non-catalytic and catalytic fast pyrolysis of corncob in a fluidized bed reactor. Bioresour Technol 2009;100:1428–34. http://dx.doi.org/10.1016/j.biortech.2008.08.031.

[86] Mante OD, Agblevor FA, Oyama ST, McClung R. The influence of recycling non-condensable gases in the fractional catalytic pyrolysis of biomass. Bioresour Technol 2012;111:482–90. http://dx.doi.org/10.1016/j.biortech.2012.02.015.

[87] Smith AR, Klosek J. A review of air separation technologies and their integration with energy conversion processes. Fuel Process Technol 2001;70:115–34. http://dx.doi.org/10.1016/S0378-3820(01)00131-X.

[88] Keoleian GA, Volk TA. Renewable energy from willow biomass crops: life cycle energy, environmental and economic performance. CRC Crit Rev Plant Sci 2005;24:385–406. http://dx.doi.org/10.1080/07352680500316334.

[89] DEFRA. Conversion factors for company reporting: methodology paper for emission factors. London UK; 2013.

[90] European Commission. C 160/8 communication from the commission on the practical implementation of the EU biofuels and bioliquids sustainability scheme and on counting rules for biofuels. Brussels, Belgium; 2010.